LARGE EDDY SIMULATION AROUND 2-D AIRFOIL WITH NATURAL TRANSITION AT HIGH REYNOLDS NUMBERS

Takuji Kurotaki*, Takahiro Sumi* and Takashi Atobe*
***Aerospace Research and Development Directorate, Japan Aerospace Exploration Agency**

Keywords: *Subsonic Flow, Transition, Unsteady Flow, LES, CFD*

Abstract

A new approach for the analysis of subsonic flow is proposed and the capability of capturing the detail flow properties is investigated. Especially, the natural transition phenomenon is focused on. The flows around two-dimensional aerofoil of the NACA0012 under relatively high Reynolds number conditions (Re ≃ 10^6) are analyzed. The development of so called T-S wave and the laminar-turbulent transition are clearly captured. Locations of transition points are compared with the experiments and agreements are excellent. The detail comparison with the linear stability analysis indicates that the most unstable disturbance in the linear unstable region is captured quantitatively by taking care of grid resolution in the chord direction. The disturbance distribution inside the boundary layer in the transitional region is examined and the phase jump is also captured.

1 Introduction

Recently, high-accuracy and high-resolution finite different schemes are widely used in many applications such as problems of aeroacoustics and the stall of an airfoil and so forth. These flows often require accurate unsteady treatments with, for example, turbulence, transition from laminar to turbulent boundary layer, flow separation and flow compressibility. Direct numerical simulations are seemingly possible only for simple geometries at low Reynolds numbers even in near future. Therefore, less expensive methods such as Large Eddy Simulations (LES) are promising approach for high Reynolds number flows with more complex geometries. However, getting quantitatively acceptable results for them are still now challenging.

Rapid advances in higher-order LES computation method have enabled us to analyze such complicated flow phenomenon around relatively complicated geometries. One of examples is Computational Aeroacoustics (CAA) in high-Reynolds number flows. Even the direct capturing infinitesimal sound wave is feasible by solving the unsteady compressible Navier-Stokes equations, which is sometimes referred to as Direct Noise Computations (DNC) [1]. Therefore, improvements of numerical methods and detail validation of them are now very important.

In this paper, a new approach for the analysis of subsonic flow is proposed, in which LES with ADM (Approximate Deconvolution Model) [2] are combined with the generalized characteristic interface conditions [3] for singular lines in a grid and the generalized Navier-Stokes characteristic boundary conditions and so on. Other numerical techniques used in this approach are selected in order to treat complex flow properties around a complex shape by the use of least number of grid points as possible.

By this approach, the capability of capturing the detail flow properties is investigated. Especially, the natural transition phenomenon is focused on. The flows around two-dimensional aerofoil of the NACA0012 under relatively high Reynolds number conditions (Re≃ 10^6) are analyzed. Locations of transition points are compared with the experiments and the detail comparison with the linear stability analysis is discussed.

2 Numerical Method

In this study, the three-dimensional compressible Navier-Stokes equations are employed as the basic equations. For the flow containing turbulence and transition, ADM type approach originally developed by Stolz et. al. [2] is used. In this method, an approximation to the unfiltered solution is obtained from the filtered solution by the series expansion of deconvolution operator. The effect of smaller scales than the filter width is modeled by a relaxation regularization including a dynamically estimated relaxation parameter.

In practical computations with structured grid, singular points can be frequently found where an abrupt grid change exists. These singularities pose troublesome problems especially when high order and high resolution scheme is applied. An excellent theory was proposed [4], which solves the above singular problem by decomposing a computational domain along a line or surface containing the singular points and by imposing accurate characteristic-based interface conditions at the interface. However, the original theory has limitations on the combination between the adjacent computational coordinate definitions, and these two coordinates have to be the same direction and the same coordinate index. A new generalized theory has been proposed by authors [3] for more flexible coordinate arrangement. This theory is applied to the region around a trailing edge when a flow around an airfoil is solved with a C-type single mesh.

Other aspects such as the computation of spatial derivatives, time integration and boundary conditions are also considered to attain high-accuracy and high-resolution schemes as a whole. The spatial derivatives of the inviscid and viscous flux terms are solved by the optimized 6th order tri-diagonal (OSOT) compact scheme suggested by Kim et al. [5], [6]. For the time integration, the low storage type of 2-step 4th order low-dissipation and low-dispersion Runge-Kutta (LDDRK) scheme (the first step is a 5-stage scheme and the second step is a 6-stage scheme) proposed by Hu et al. [7], [8] is used. This scheme increases numerical stability in the explicit time integration, and reduces the dissipation and dispersion errors simultaneously. CFL=1 is used throughout this study. For the inflow, outflow and wall boundary conditions, the Navier-Stokes characteristic boundary conditions (NSCBC) extended to the generalized coordinate system by Kim et al. [9], [10] are applied. The forced damping of waves with the sponge method near the outer boundary [11] is also applied combined with the implicit damping through the extension of grid intervals in the direction from body to outer boundary.

3 Results and Discussions

3.1 Experiments and Numerical Conditions

In this study, the flow around two-dimensional airfoil of the NACA0012 under relatively high Reynolds number condition is studied.

The flow conditions and the dimensions of the airfoil are according to the experiments by Tokugawa et.al. [12]. In the experiments, the location of the natural location was examined in detail for the NACA0012 in low-speed wind tunnel facilities. The chord length of the airfoil was 1.0 m and the angle of attack was 0 degree. The transition locations were detected by three independent approaches; the non-dimensional dynamic pressure measurements by Preston tubes, the local velocity fluctuation measurements by hot wires and the measurements of the surface temperature distribution by the use of infrared cameras. The estimated locations by these methods agreed well in the different two wind tunnels; the Large-scale low-noise wind tunnel of Railway Technical Research Institute and Low-speed wind tunnel in Japan Aerospace Exploration Agency referred to as “RTRI” and “LWT1” respectively in the following.

Three cases are selected according to the different chord wise grid spacing in transition region near wall surface for this numerical research. The numerical conditions for each case are summarized in Table 1.

For the 30 m/s case in Case 3 conducted as a preliminary calculation, the results of linear stability analysis with the averaged flow profiles did not coincide with the results directly obtained from the data of fluctuating velocity of LES. The most amplified frequency of the unstable disturbance in the transition area from the linear stability analysis was about 700Hz at 40% chord length, whereas the fluctuating data showed about 200Hz. The frequency with the peak spectrum in the wind tunnel tests at 50% chord also supported the analytical value showing about 600Hz.

For the Case 3, the averaged grid intervals in this direction around 50% chord length was about 17mm near the surface. If we assume the phase velocity of the unstable disturbances is about 40% of the uniform velocity, the estimated wavelength corresponding to 600Hz is about 20 mm. So, the possible reason of the disagreements in the Case 3 was expected because the grid resolution in the chord wise direction was not enough to capture these disturbances. In the grid for the Case 2, the averaged grid interval is reduced to about 6 mm with which the wavelength of disturbances can be captured with better resolution than the Case 3. For the Case2, better results were obtained as expected. The frequency spectrum of velocity fluctuation was almost comparable to the experimental data. However, the frequency of the most unstable disturbance in the linear unstable region was still slightly underestimated; the numerical flow result had a peak at about 400 Hz at 40% chord length.

These observations show that the numerical resolution in the transitional region is very important and the result can be improved with finer grid intervals there. So, the averaged grid interval is reduced further to about 2.7 mm. We call this case as "Case 1" .

Table 1 Summary of Numerical Conditions.

	Case 1	Case 2	Case3
Aerofoil	NACA0012		
Chord length: c	1.0m		
Angle of attack: α	0 degree		
Uniform flow velocity: U_∞	15, 30 m/s	15, 30 m/s	15, 20, 25, 30 m/s
Reynolds number: Re_∞	2.2×10^6 for 30 m/s		
Total grid points (circumferential × radial × spanwise)	3.6 million (1001 × 71 × 51)	3.6 million (1001 × 71 × 51)	3.7 million (601 × 121 × 51)
Spanwise length	0.125 c	0.125 c	0.25 c
Radial grid spacing on the wall surface	$1\times10^{-4}c$	$2\times10^{-4}c$	$2\times10^{-4}c$
Chord wise grid spacing in transition region near wall surface	2.7 mm	6 mm	17 mm

3.2 Numerical Results and Comparison with Experiments

Fig. 1 shows the contour of instantaneous vorticity of the spanwise component $-\omega_z$ at 0.8 mm away from the wall for the Case 1 to 3. As can be seen from these figures, the so-called 2-D T-S wave is growing at the beginning of the boundary-layer transition near the leading edge and then is deformed into the peak-valley structure due to the secondary instability, resulting in amplifying oblique T-S waves. This process agrees with the scenario of 2-D boundary-layer transition observed in the low turbulence uniform flow.

In the experiments, the location of transition points from laminar to turbulent flows was determined by the three independent approaches as mentioned above. Among them, two approaches through the dynamic pressure and surface temperature measurements are based on the analogy with the abrupt increase of the wall friction coefficient c_f at the transition area. In this study, therefore, it is convenient to use the c_f directly calculated from the numerical results in order to compare the transition points with the experiments.

The definition of the transition points is as follows. Firstly the c_f line is extrapolated by three different lines. Two intersections usually appear along the c_f curve. Then one of the intersections close to the leading edge is defined as "the onset of transition." Whereas, the intersection close to the trailing edge is defined as "the end of transition." Finally, the transition location is defined as the middle point of those two intersections. In Fig. 2, the distributions of c_f are presented for the 15 and 30 m/s cases of the Case 1 with three extrapolated lines.

Fig. 3 shows the top view of the contour map for the cases corresponding to Fig. 1. The uniform flow comes from the left hand side and the indices on the top of the figures denote the chordwise location under the normalization with the chord length. Three arrows put on the each case denote locations of the onset, the transition, and the end, respectively. In this figure, it is shown that each arrow goes to upstream with the increase of the uniform flow velocity. This forward shift of the transition location with the increase of the Reynolds number is quite reasonable.

The transition points estimated under the same definition mentioned above are compared with the experimental results as shown in Fig. 4. The vertical line x_{Tr}/c in this figure is a non-dimensional transition location from the leading edge. Two kinds of experimental results are presented here according to the independent two wind tunnels; “RTRI” and “LWT1”. Three data for each experiments corresponding to different approaches of measurements mentioned above are shown in the figure. The discrepancy between the experimental results in two wind tunnels is caused by the difference of the turbulent level. This level for “RTRI” symbolized by triangle is about 0.05%, whereas that for “LWT1” symbolized by circle is about 0.15%. The transition location generally moves forward when the turbulent level increases, therefore, this discrepancy seems reasonable.

The estimated transition points from CFD results for each case for the 30 m/s case are delayed slightly from those in the experiments, which also seems reasonable because the turbulent energy level is considered quite small in CFD. These overall results show that the transition locations themselves agree well with experiments, especially for “RTRI”, and the effect of difference of the grid interval in the transition region between the Case 1 and 2 is not noticeable.

Fig. 5 is the detail of the power spectrum density distributions of unstable waves at mid-span for the 30 m/s case of the Case 1 at each chord wise locations from x/c = 0.05 to 0.5. The stream wise velocity u at 0.8mm distant from wall surface is analyzed here. These figures show the development of unstable flow region

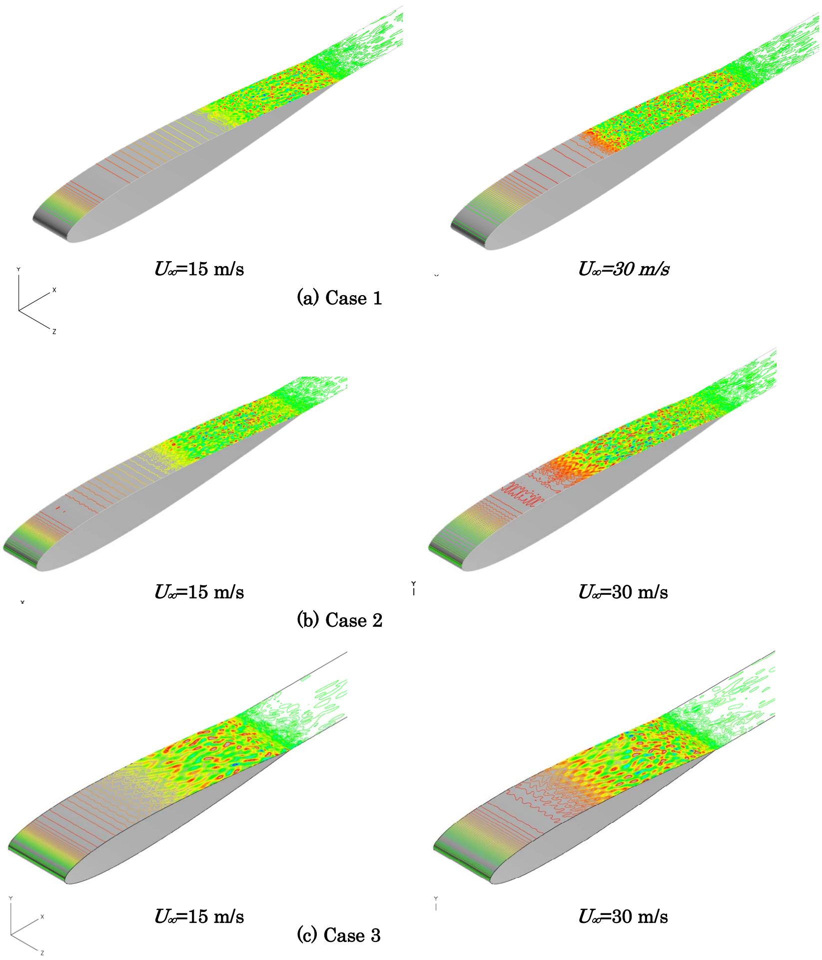

Fig. 1 Instantaneous Vorticity $-\omega_z$ (0.8 mm away from the wall).

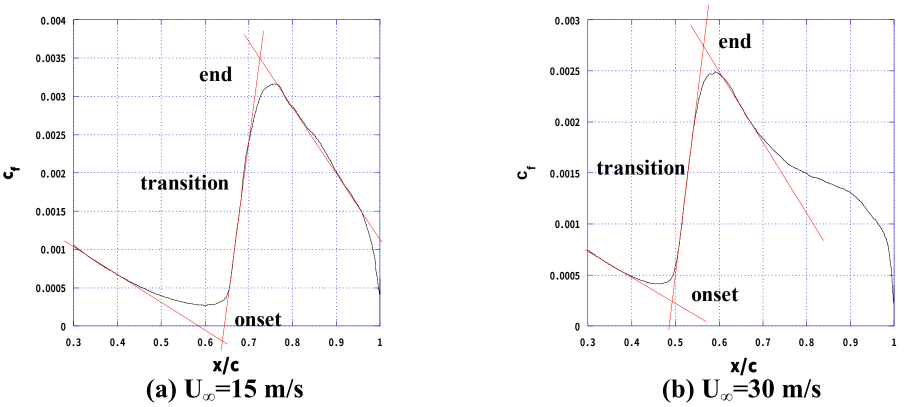

Fig. 2 Wall Friction Coefficient Distribution and Definition of Transition Point. (Case 1)

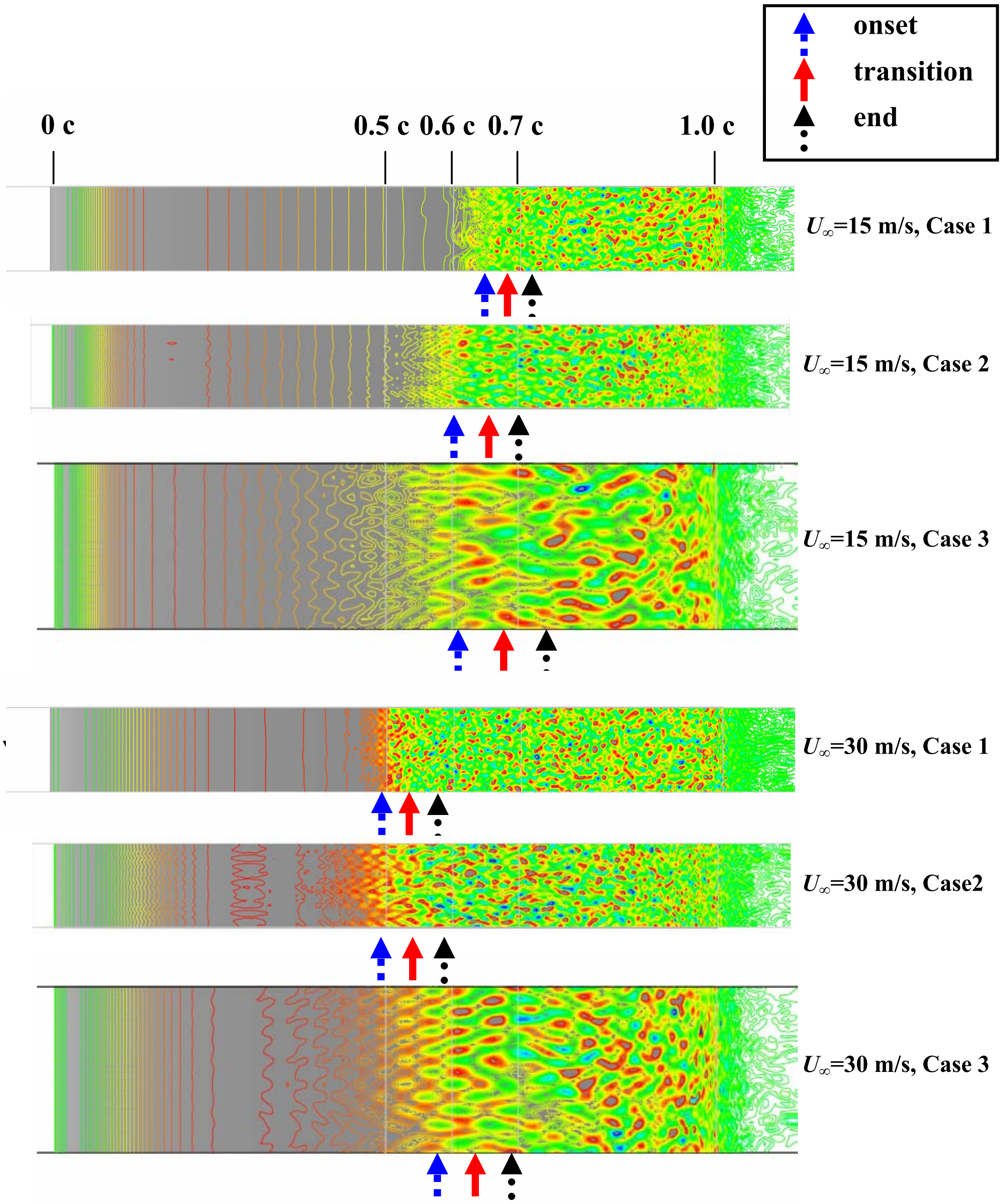

Fig. 3 Transition Location for Each Cases. (Contour is the same as in Figure 2.)

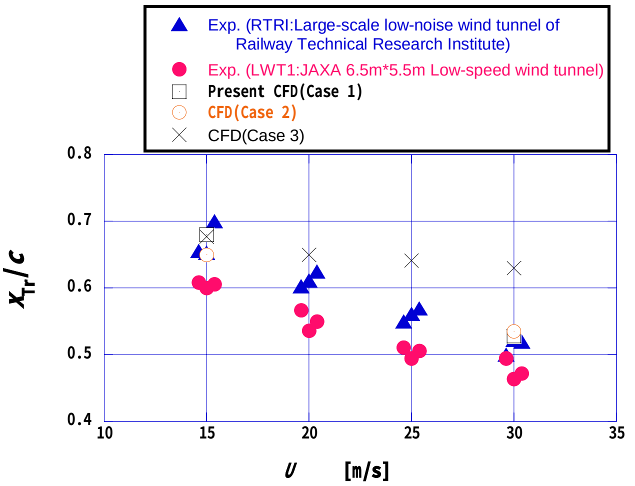

Fig. 4 Comparison of transition locations for each cases.

before the transition point well. The prominent increase of amplitude begins between x/c = 0.2 and 0.3. The frequency with the peak spectrum at 40% chord is observed around 700 Hz in Fig. 5 (f).

3.3 Comparison with Linear Stability Analysis

In order to validate the present results more quantitatively, the linear stability analysis based on the e^N method is conducted. The averaged velocity profile inside the boundary layer directory obtained from the present numerical result is used as input data. In this study, only the numerical results for U_∞= 30 m/s, Case 1 is shown. Another independent approach is also tried for the same case by the famous Kaups-Cebeci manner [13] and SALLY code [14] for the comparison of the velocity profile and its stability, respectively.

First of all, how to obtain the N factor, which corresponds to the amplitude of small disturbance propagating inside the boundary layer, is roughly explained here. The amplification rate of the small disturbance at each stream wise location is estimated using the common Orr-Sommerfeld equation,

$$\frac{1}{Re_{\delta^*}}(D^2-\alpha^2)^2\,\overline{w}+i(\omega-\alpha U)(D^2-\alpha^2)\overline{w}+i\alpha D^2U\overline{w}=0 \tag{1}$$

This equation is derived by the substitution of the following plane wave solution of small disturbance represent as Eq. (2) into the disturbance equation, which is obtained from the basic equation describing the flow field under the two dimensional parallel flow assumption with the unsteady small disturbance,

$$\boldsymbol{u}=\overline{\boldsymbol{u}}(y)\exp\{i(\alpha x-\omega t)\} \tag{2}$$

In Eq. (1) and (2), α denotes a complex wave number, ω a real frequency of the disturbance and U mean velocity in the tangential direction along the surface. $\overline{w}$ is the normalized disturbance of velocity in the orthogonal direction and $\overline{\boldsymbol{u}}(y)$ denotes a vector consists of the small disturbance in the linearized disturbance equations. The growth rate of the disturbance wave depends on the sign of the imaginary part of wave number α_i. Namely, the amplitude of the disturbance wave increases with the increase of x if the sign of the imaginary part of wave number is negative. In other words, the disturbance wave is stable when α_i is positive, and unstable when α_i is negative. Since the disturbance wave develops in the exponential manner under the present assumption, its intensity is usually estimated by e^N method which was proposed by Smith and Gamberoni [15] and Van Ingen [16], and the definition of the N factor is given as following,

$$N \equiv \ln(A/A_0) = -\int_{x_0}^{x_1}\alpha_i dx \tag{3}$$

A_0 denotes the initial amplitude of the disturbance wave at location x_0, and A denotes amplitude at x_1. In general, the laminar-turbulent transition occurs when this N factor reaches to around 12-15 at the location of the corresponding x_1.

In order to calculate the N factor, the complex wave number α at each chord wise location has to be obtained by Eq. (1) as a function of the frequency ω of the disturbance wave. Then integrating the α_i along to x direction, the growth of the N factor is obtained for each frequency. Usually, how define the location x_0 as initial position is an important problem. Here x_0 is defined as the neutral point which corresponds to the position changing the sign of α_i from positive to negative.

Results of the linear stability analysis for disturbance waves with typical frequencies (200-1,000Hz) are shown in Fig. 6 for the Case1.

It can be seen from this figure that in the leading edge region up to x/c = 0.15, the flow is stable and transfers to unstable area where the N factor increases. Furthermore, the critical point, which the stability changes from stable to unstable, moves upstream with the increase of the frequency of the disturbance. N factor for the disturbance with 700Hz obtained by the SALLY code is also shown in the same figure. These two lines corresponding to this frequency almost coincide with each other at least before x/c = 0.35, but become separate thereafter. So, the influence of nonlinearity begins to appear around there. Finally the slope of the N factor for the numerical result decreases around the half chord position where the boundary-layer transition is supposed to begin. The corresponding N factor to the transition location from the numerical result in this case is about 12.5 by the SALLY code, which coincides with the general criteria used for the estimation of the transition points by the linear stability theory.

In general, the frequency of the most unstable disturbance varies at each chord wise locations. The N factor as a function of the frequency is shown in Fig. 7 for two different locations at x/c = 0.4 and 0.5. From this figure, the range of unstable region can be estimated and the most unstable disturbance also can be known. At the position of x/c = 0.4, the most unstable disturbance is of about 700Hz. Then the peak changes to lower frequency at the position of x/c = 0.5 and its value is about 600Hz.

These results from the linear stability analysis can be used to discuss the quality of the numerical results directly obtained from the unsteady calculation for U_∞= 30 m/s, Case 1. It can be clearly seen from Fig. 6 that the disturbance levels between 200 and 1,000Hz decrease up to x/c = 0.15 and this tendency can be also observed in Fig. 5 (a), (b) and (c), which indicates that the flow is in the stable region. On the other hand, Fig. 5 (e), (f) and (g) show that amplitudes of the disturbances increase and that lower frequencies slightly delay, which corresponds to the linear stability analysis in the range from x/c=0.3 to 0.5 as in Fig. 6.

3.4 Disturbance Distribution in Boundary Layer and Formation of Oblique Wave

In the foregoing discussion, it is shown that the results of this CFD analysis can explain the development of 2-D T-S wave and that the frequency of the most unstable disturbance in the linear unstable region is captured quantitatively. Here, the characteristics of disturbance distribution inside the boundary layer are examined.

In Fig. 8 (a), the disturbance amplitude of streamwise velocity for U_∞=30 m/s case at x/c=0.4 for Case 1 is shown. The root mean square of disturbance amplitude is normalized to its inner maximum value in this figure. There exist the inner and the outer amplitude maximum inside the boundary layer. The phase profile is also show in Fig. 8 (b) .The phase jump is clearly observed near the amplitude maximum. These are the typical characteristics observed in near wall flows on the flat plate in lower Reynolds number region [17].

Fig. 1 indicates that just before the transition, the amplifying oblique T-S waves exist and that the region of them becomes smaller as the grid interval in the chord direction in CFD decreases, namely, as the solution approaches the real situation. The streamwise velocity fluctuation $u-\bar{u}$, around the transition region for U_∞=30 m/s case, Case 1 are shown in Fig. 9. This figure indicates that the amplifying oblique T-S waves are formed just after x/c=0.4. Up to x/c=0.4, the wave is almost two-dimensional and the wavelength directly estimated from Fig. 9 is about 18 mm.

In this case where the grid spacing is rather coarse, no more expected detail structures such as Λ-vortices are observed. However, the results of good agreement of the transition locations with experiments indicate that the LES approach used here can simulate the location of the natural transition with rather coarse grid points without capturing completely detail transitional flow structures.

4 Conclusion

A new approach for the analysis of subsonic flow is proposed and the capability of capturing the detail flow properties is investigated both qualitatively and quantitatively. Especially, the natural transition phenomenon around the two dimensional airfoil is focused on.

The flow around two-dimensional aerofoil of the NACA0012 under relatively high Reynolds number condition ($Re \simeq 10^6$) are analyzed with the 3.5 million grid points. In this study, care is taken for grid intervals in the chord wise direction of the transition region. It is shown that the development of so called T-S wave and the laminar-turbulent transition are clearly captured. The locations of these transition points obtained from numerical results are compared with the experiments and agreements are excellent.

The detail comparison with the linear stability analysis indicates that the most unstable disturbance in the linear unstable region is captured quantitatively by taking care of grid resolution in the chord direction.

The characteristics of disturbance distribution inside the boundary layer in the transitional region are also examined. There exist the inner and the outer amplitude maximum inside the boundary layer and the phase jump is also captured. These are the typical characteristics observed in near wall flows on the flat plate in lower Reynolds number region.

References

[1] O. Marsden, C. Bogey and C. Bailly. Direct Noise Computation around a 3-D NACA 0012 airfoil. *AIAA paper* 2006-2503, 2006.

[2] Stolz, S., Adams, N. A., and Kleiser, L. The approximate deconvolution model for LES of compressible flows and its application to shock-turbulent-boundary-layer interaction. *Phys. Fluids*, Vol. 13, pp. 2985-3001, 2001.

[3] Sumi, T., Kurotaki, T.and Hiyama, J. Generalized characteristic interface conditions for high-order multi-block computation. *International Journal of Computational Fluid Dynamics*, Vol. 21, pp. 335-350, 2007.

[4] Kim, J, and Lee, D. Characteristic Interface Conditions for Multiblock High-Order Computation on Singular Structured. Grid. *AIAA Journal*, Vol. 41, pp. 2341-2348, 2003.

[5] J. Kim and D. Lee. Optimized Compact Finite Difference Schemes with Maximum Resolution. *AIAA Journal*, Vol. 34, pp. 887-893, 1966.

[6] J. Kim and D. Lee. Implementation of Boundary Conditions for Optimized High-Order Compact Schemes. *Journal of Computational Acoustics*, Vol. 5, pp. 177-191, 1997.

[7] F. Hu, M. Hussaini and J. Manthey. Low-Dissipation and Low-Dispersion Runge-Kutta Schemes for Computational Acoustics. *Journal of Computational Physics*, Vol. 124, pp. 177-191, 1996.

[8] D. Stanescu and W. Habashi. 2N-Storage Low Dissipation and Dispersion Runge-Kutta Schemes for Computational Aeroacoustics. *Journal of Computational Physics*, Vol. 143, pp. 674-681, 1998.

[9] Kim and D. Lee. Generalized Characteristic Boundary Conditions for Computational Aeroacoustics. *AIAA Journal*, Vol. 38, pp. 2040-2049, 2000.

[10] J. Kim and D. Lee. Generalized Characteristic Boundary Conditions for Computational Aeroacoustics, Part 2. *AIAA Journal*, Vol. 42, pp. 47-55, 2000.

[11] T. Colonius. Modeling Artificial Boundary Conditions for Compressible Flow. *Annual Reviews of Fluid Mechanics*, pp. 315-345, 2004.

[12] Tokugawa, N., Takagi, S, et al. Influence of External Disturbances on Natural Boundary-Layer Transition in 2-D Wing Flows. *J. Jpn Soc. Fluid Mech*., Vol. 22, No. 6, pp. 485, 497, 2003.

[13] Kaups,K., and Cebeci,T. Compressible Laminar Boundary Layers with Suction on Swept and Tapered Wings. *J.A*,, Vol. 14, No. 7, pp.661, 1977.

[14] Strowski,A., and Orszag,S. Mass Flow Requirements for LFC Wing Design. *AIAA Paper* 77, pp.1222, 1977.

[15] Smith,A.M.O. and Gamberoni,N. Transition, Pressure Gradient and Stability Theory. *Douglas Aircraft Co.Rept.* ES 26388, El Segundo, California, 1956.

[16] Van Ingen,J.L. A Suggested Semi-empirical Method for the Calculation of the Boundary Layer Transition Region. *Univ.of Techn.,Dept.of Aero.Eng.Rept.*UTH-74, Delft , 1956.

[17] A. V. Boiko, G. R. Grek, A. V. Dovgal and V.V. Kozlov. *The Origin of Turbulence in Near-Wall Flows.* Springer-Verlag , 2002.

Copyright Statement

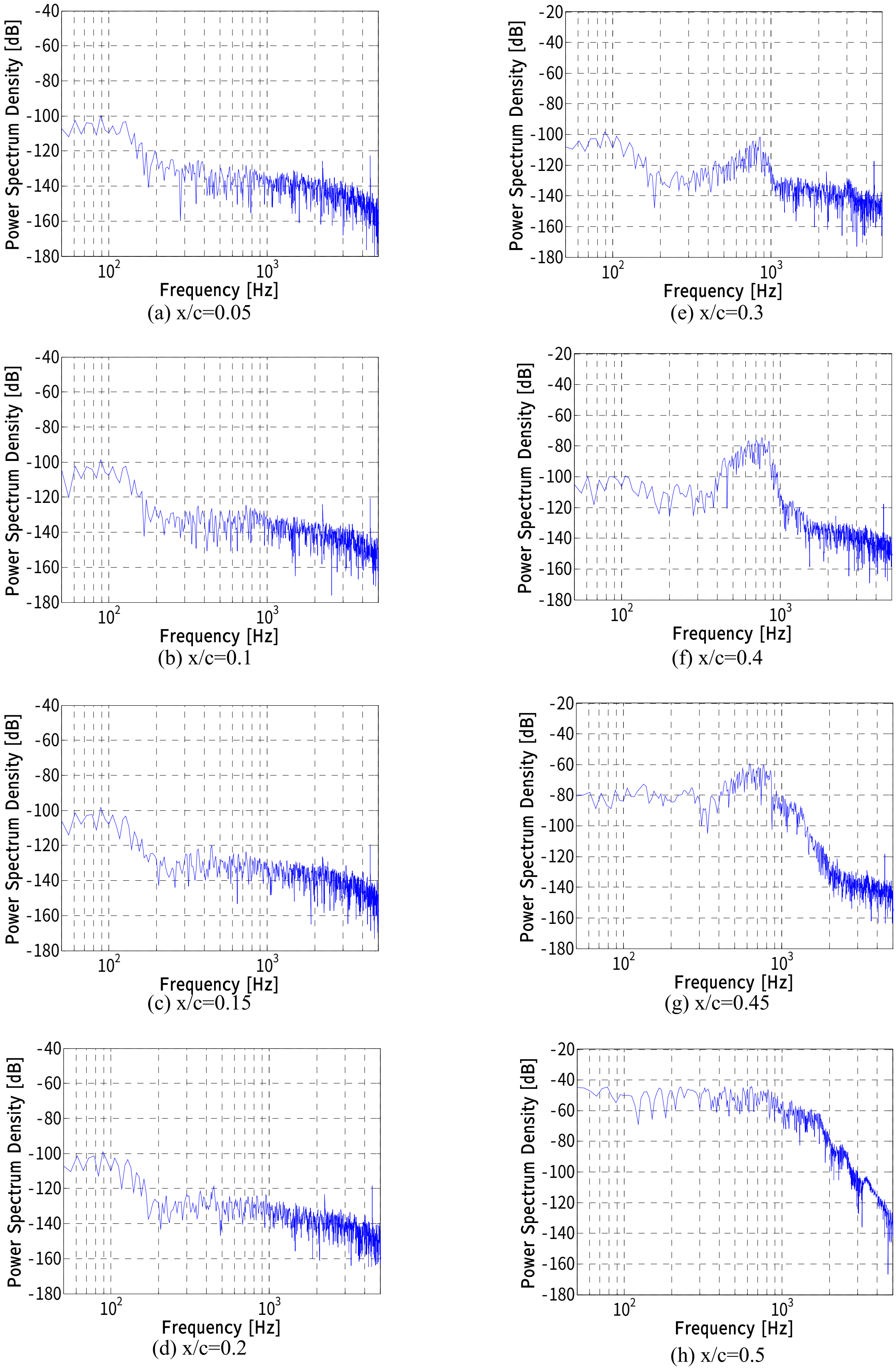

Fig. 5 Power Spectrum Distribution of Unstable Waves for Case A (U=30 m/s, streamwise velocity fluctuation at 0.8mm distant from wall surface)

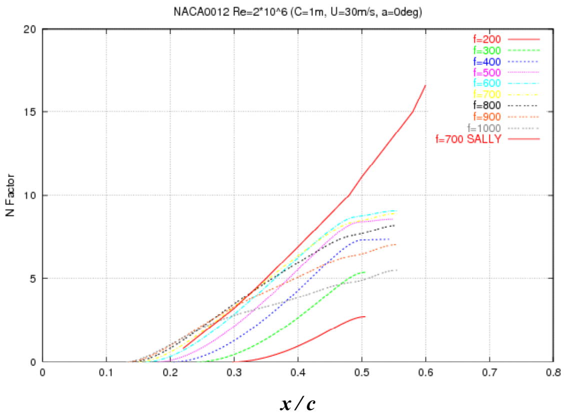

Fig. 6 Variation of N Factor with Chord Wise Location *x / c* for Case1.

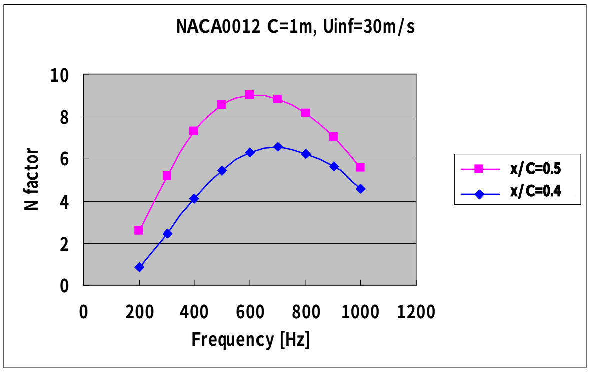

Fig. 7 Variation of N Factor with Ffrequency at x */c* = 0.4 and 0.5 for Case 1.

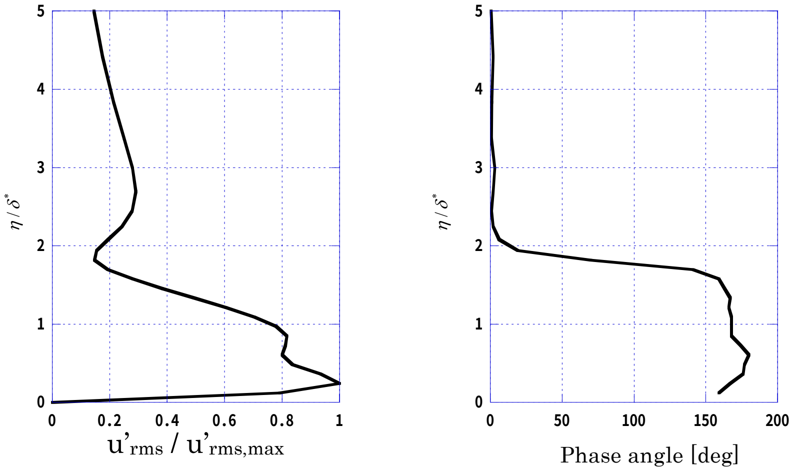

(a) Disdurbance amplitude

(b) Phase angle

Fig. 8 Disturbance Amplitude of Streamwise Velocity and Phase Distributions at 700Hz for U_∞=30 m/s Case at x/c=0.4 for Case 1.

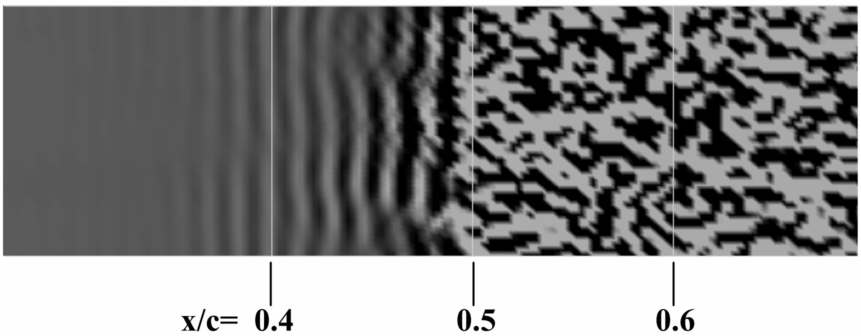

Fig. 9 Streamwise Velocity Fluctuation **u -ū** for U_∞=30 m/s Case, Case 1. (0.8 mm away from the wall)